A damped decadal oscillation in the North Atlantic climate system

Carsten Eden and Richard J. Greatbatch

Dalhousie University, Halifax, Canada

revised Manuscript, re–submitted to Journal of Climate at Feb 28, 2003.

Corresponding author address:

Carsten Eden

Institut für Meereskunde,

FB I, Theorie und Modellierung

Düsternbrooker Weg 20

24105 Kiel, Germany

email: ceden@ifm.uni-kiel.de

All figures are available in electronic format.

Abstract

A simple stochastic atmosphere model is coupled to a realistic model of the North Atlantic Ocean. A north–south SST–dipole with its zero line centered along the subpolar front, influences the atmosphere model which in turn forces the ocean model by surface fluxes related to the North Atlantic Oscillation. The coupled system exhibits a damped decadal oscillation associated with the adjustment through the ocean model to the changing surface forcing. The oscillation consists of a fast wind-driven, positive feedback of the ocean and a delayed negative feedback orchestrated by overturning circulation anomalies. The positive feedback turns out to be necessary to distinguish the coupled oscillation from that in a model without any influence from the ocean to the atmosphere. Using a novel diagnosing technique, it is possible to rule out the importance of baroclinic wave processes for determining the period of the oscillation, and to show the important role played by anomalous geostrophic advection in sustaining the oscillation.

1 Introduction

In the North Atlantic sector, climate variability with time scales from months to decades is dominated by the North Atlantic Oscillation (NAO) (Wallace and Gutzler, 1981); that is the simultaneous strengthening (weakening) of the Icelandic Low and the Azores high, and concomitant strengthing (weakening) of the prevailing westerly winds. The influence of the NAO on Eurasian and North American climate is well established and has been documented, for example, by Hurrell (1996), Kushnir (1999), Greatbatch (2000) and Lu and Greatbatch (2002). Clearly, longer–term prediction of the NAO, beyond the time scale of traditional weather forecasts, could yield considerable socio–economic benefit for Europe and North America.

Among the possible candidates to extend prediction of the NAO is the ocean with its long–term memory imprinted in sea surface temperature (SST) anomalies (Bjerknes, 1964). It remains unclear, however, from which region the most important impact of SST anomalies on the NAO originates. Different model simulations (e.g. Molteni and Corti (1998); Rodwell et al. (1999); Hoerling et al. (2001); Robertson et al. (2000); Cassou and Terray (2001)) and observational analyses (e.g. Czaja and Frankignoul (2002); Rodwell and Folland (2002)) give different answers. Here we concentrate on the possible influence of the mid–to high–latitude North Atlantic on the NAO that is supported by the work of Rodwell et al. (1999), Czaja and Frankignoul (2002) and Rodwell and Folland (2002), but we note by doing so, we do not question the possible influence of, e. g. tropical SST anomalies in forcing the NAO as well (e. g. Hoerling et al. (2001); Peterson et al. (2002)).

If the ocean is to be used to extend prediction of the NAO, then the ocean SST must itself be predictable. Several authors (Rodwell et al., 1999; Mehta et al., 2000; Hoerling et al., 2001; Latif et al., 2000) have shown that atmospheric general circulation models (AGCM's), forced by the historical record of SST and sea-ice extent, can reproduce, in an ensemble mean sense, the observed NAO index (NAOI) on time scales beyond about 6 years. On the other hand, Bretherton and Battisti (2000) have shown with a simple stochastic model (BB model), that this result could be interpreted as the

ensemble mean response of the AGCM to the integrated weather noise archived in the SST, which would reduce the potential predictability of the NAO drastically to at most a few months. However, in a precursory study to the present one, Eden et al. (2002) have shown that replacing the oceanic part of the BB model with a realistic oceanic general circulation model (OGCM) changes the system in a way that a damped decadal oscillation becomes possible. Eden et al. (2002) showed that the presence of the damped oscillation provides some potential predictability of the NAOI up to a decade into the future for certain initial states of the ocean.

The ocean model used by Eden et al. (2002) is essentially the same as in Eden and Jung (2001) and Eden and Willebrand (2001). Those papers describe the performance of the model in comparison with observations. They find that the model has skill at simulating the observed time evolution of SST in the North Atlantic on time scales from interannual to interdecadal when driven by realistic surface forcing, and that the evolution of the SST anomalies is partly driven by the changing circulation in the model. Beismann et al. (2002) and Gulev et al. (2003) have shown that similar North Atlantic models reproduce essentially the same results as the above models, and Häkkinen (1999, 2001) has also shown that realistic forcing of a different OGCM has skill at simulating SST in the North Atlantic. Using a surrogate model that mimics the behavior of the OGCM coupled to the BB model atmosphere, Eden et al. (2002) show that their simple coupled system has skill at predicting SST on time scales out to a decade (see Figure 3 in their paper). For these reasons, we believe the damped oscillatory behavior noted by Eden et al. (2002) is relevant to the North Atlantic Ocean, and, in particular, to the response of the North Atlantic Ocean to changes in the surface forcing.

In the present study, we examine the damped decadal oscillation described by Eden et al. (2002) in detail and describe the mechanism by which the wind and thermohaline driven circulation act to support the oscillation. Several theories concerning the variability of the North Atlantic circulation and its interplay with the NAO have been proposed; focusing on oceanic baroclinic wave dynamics (e.g. Marshall et al. (2001); Johnson and Marshall (2002)), or on simple advective processes (e.g. Saravanan and McWilliams (1997)). In addition, Dewar (2001) has suggested the importance of non-

linear processes associated with mesoscale eddies in the ocean for driving variability in the SST and the overlying atmosphere. Eden and Willebrand (2001) and Eden and Jung (2001) found that variability in the thermohaline circulation (THC) plays an important role in the dynamical response to variability in the atmospheric forcing related to the NAO. Eden and Willebrand (2001) speculated that (viscous) boundary waves play a role in variability of the THC. Döscher et al. (1994) noted the importance of boundary waves in the response of a North Atlantic model to a change in the high latitude forcing, whereas Gerdes and Köberle (1995), and a number of other authors (e. g. Marotzke and Klinger (2000); Goodman (2001)), have noted the importance of advective processes in the adjustment of ocean models to changes in high latitude forcing. Here we are able to answer the question as to the importance of wave dynamics compared to other processes, such as advection, by using a novel technique for diagnosing OGCM's. It turns out that the previous speculations about (boundary) wave dynamics do not apply in our coupled model, but advective processes, both mean and anomalous, play an important role.

This paper is structured as follows: In section 2 we describe the damped decadal oscillation in the coupled model and in section 3 we describe the mechanism of this oscillation with a focus on the period and the damping time scale. The last section will give a concluding discussion of our findings. We have added two appendices where more technical descriptions and model details are given.

2 The damped oscillation

2.1 Model set-up and experiments

To start, we want to briefly introduce the coupled model. Readers are referred to Appendix A for a more detailed description of the model and the coupling procedure. The OGCM is part of the FLAME hierarchy of models, which have been used with good success in, e.g. Eden and Jung (2001) and Eden and Willebrand (2001) to simulate interannual to interdecadal variability in the North Atlantic. The OGCM is coupled to a simple stochastic atmosphere described by Bretherton and Battisti (2000) (BB model). The original BB model is formulated as a simple heat balance for the lower atmosphere (T_a)

and the upper, mixed layer of the ocean (T_o). The unpredictable atmospheric weather is specified as a stochastic variable (N) with a Gaussian distribution characterized by mean zero and variance one (white noise); i.e.

$$\dot{T_a} = bT_o - aT_a + N \quad , \quad \beta\dot{T_o} = cT_a - dT_o$$

(Parameters take the same values and meanings as in Bretherton and Battisti (2000)). To relate the BB model to reality, especially the NAO, it is possible to interpret T_a as the NAOI and T_o as a certain SST–index for the North Atlantic (Bretherton and Battisti, 2000; Marshall et al., 2001). We have replaced the simple mixed layer ocean in the original BB model with the more realistic OGCM by taking T_o as a projection of SST anomalies produced by the OGCM on to the fixed SST (feedback) pattern described in Appendix A and shown in Figure 13. Associating T_a with the NAOI, we then force the OGCM with NAO–related surface heat flux and wind stress anomalies, as in Eden and Jung (2001) and Eden and Willebrand (2001). The ocean is able to feedback on T_a, the NAOI, by the term bT_o in the tendency equation for T_a in both the original BB model and our modified setup.

As discussed in Eden et al. (2002), the dynamical response of the ocean to the NAO forcing constitutes a significant change in the characteristics of the coupled system compared to the original BB model. In particular, changes in the ocean circulation in response to the forcing variability changes the oceanic heat transport in a way that affects the SST. In the North Atlantic, changes in heat transport are associated with changes in the thermohaline driven (overturning) circulation (Böning et al. (1995), Eden and Jung (2001) and Eden and Willebrand (2001)). It appears therefore natural to relate the variability in the coupled model to a certain overturning (THC) index. We choose as this index the value of the meridional streamfunction at mid depth ($\sim$ 1270 m) near the intergyre boundary ($\sim 47.9^o$ N) where the climatological maximum overturning is located in this model,

We utilize three different experiments with the OGCM to discuss the separate influence of the forcing functions (wind stress versus heat flux) and the feedback from the OGCM to the atmosphere (coupling parameter b). Here is a list of the principal experiments to be discussed:

- A 200 year long integration of the OGCM coupled to the BB model. This experiment is called STANDARD
- A 100 year long integration in which we have excluded wind stress variability. The OGCM is forced by variability in heat fluxes only, all other forcing functions remain climatological as in the spin-up phase. This experiment is called HEATONLY
- A 100 year long integration in which we have excluded any feedback from the OGCM to the BB model, i.e. $b = 0$. This experiment is called UNCOUPLED.

2.2 Model results

To begin, we show in Figure 1 time series of the atmospheric variable T_a (scaled NAOI) and the SST–index T_o for the three different experiments. Similar behavior in T_a can be seen in all three experiments, although the variance of T_a in both HEATONLY and UNCOUPLED is less than in STANDARD. This reduced variance is even more clear in the time series of T_o. The standard deviation of T_o from both HEATONLY and UNCOUPLED is less than 50% of the standard deviation of T_o in STANDARD. While T_o from STANDARD is therefore clearly distinguishable from UNCOUPLED, the time series of T_o for HEATONLY is nearly the same as in UNCOUPLED. It follows that including the wind stress forcing associated with the variable NAOI is an important aspect of the coupled model behavior. Indeed, wind stress plays an important role in the dynamics of the damped oscillation of the model. In the remainder of this section, we show how wind stress and heat flux induced variability in the ocean circulation supports changes in the SST–index T_o and, accordingly, the damped oscillation in the coupled model.

Figure 2 (left panel) relates the THC index in STANDARD to the atmospheric variable T_a by a linear, lagged regression. The figure shows significant positive regressions for negative lags of 1–5 years (with a maximum at 2–3 years) which means that a high value of T_a precedes on average a high value of the THC index by about 2–3 years. The regression coefficient at zero lag cannot be distinguished

from the null hypothesis; however, significant negative regression coefficients show up for positive lags of 2–6 years (with a maximum at about 4 years), which means that high values of the THC index precedes, on average, negative values of T_a by about 4 years. The lagged regression function shows a quite smooth, oscillatory shape with significant regressions for even higher lags, pointing towards the oscillatory and coupled behavior of both variables. The right panel of Figure 2 shows the same analysis for HEATONLY with quite similar results, although, significant positive correlations around +10 years and +20 years (ocean is leading) do not show up in contrast to STANDARD, denoting the less effective feedback from ocean to atmosphere in HEATONLY. A similar analysis for UNCOUPLED (not shown) reveals, as expected, no significant regression for positive lags (ocean is leading) and a similar but less regular behavior of the regression function for negative lags, i.e. significant (positive) regressions for -1 years to -5 years lag only.

Having now established the relation of the THC index to the forcing variability, we proceed by relating the THC index to changes in the meridional heat transport. First, we focus on the heat transport near the boundary between the subtropical and subpolar gyres, since this is where the heat transport is most effective at influencing the heat content, SST, therefore T_o and T_a. Figure 3 shows lagged regressions between the THC–index and heat transport changes at 48^oN in STANDARD. We have decomposed the heat transport into a "gyre" component and an "overturning" part [1]. The regression for the overturning part is symmetric around zero lag and very similar to the autocorrelation function of the THC–index itself (not shown). It follows that changes in the meridional streamfunction determine changes in the overturning part of the heat transport changes. The gyre part, however, shows a different temporal behavior: there is a phase shift of about 3 years ($\sim 90^o$) between the maximum of the THC–index at lag zero and the maximum of the gyre heat transport. Thus, according to Figure 2, the gyre component is in phase with the negative of the forcing T_a, suggesting that it is part of a rapid dynamical response to the forcing. Since a negative heat transport anomaly at 48^o N

[1] "Gyre" heat transport is defined (Bryan, 1962) as the (zonal) correlation of deviations from the zonal mean of meridional velocity and heat content and the "overturning" part is the product of the zonal means. However, note that this decomposition is not unique, i.e. there are other possible decompositions.

will tend to cool the subpolar and to warm the subtropical North Atlantic, we may interpret the gyre contribution as an immediate, positive feedback on T_a (via bT_o). The overturning part shows a delay of ($\sim 90^o$) with respect to T_a (Figure 2) and constitutes therefore a delayed, negative feedback on T_a.

The gyre contribution in Figure 3 is almost twice as large as the overturning part. In a corresponding regression analysis for HEATONLY, the gyre contribution is much reduced (not shown). Thus, we can relate the enhanced gyre contribution to the wind forcing. In fact, it is an effect of the topographic Sverdrup response to the wind stress forcing, noted by Eden and Willebrand (2001) (see also below). HEATONLY lacks the immediate positive feedback by the gyre heat transport and, therefore, we see much reduced variance of the damped oscillation in Figure 1. Note that Ekman heat transport [2] changes are of minor importance for this damped oscillation (see Figure 3). The likely reason is that the mean Ekman heat transport is not important in the subpolar North Atlantic compared to the other contributions (see also e.g. Böning et al. (1995) and Eden and Willebrand (2001)).

We proceed now by relating the changes in the THC–index to the basinwide changes in circulation to illustrate how these changes are able contribute to the heat transport variability noted above. We start with the meridional circulation. Figure 4 shows the pointwise regression map of the meridional streamfunction versus the THC–index in STANDARD at lags from -4 years to 4 years (index leads). The major signal is a positive anomaly, which starts to develop for lags of -4 to -1 years in the northern North Atlantic, reaching its maximal strength at zero lag and decaying for positive lags while moving further southwards. At the end of the sequence a negative anomaly shows up in the northern North Atlantic. Lags of -3 to -2 years are related to positive values of T_a (compare Figure 2) and enhanced heat loss in the subpolar North Atlantic related to a high NAO (T_a) favoring enhanced deep convection

[2]Ekman heat transport is usually defined (Bryan, 1962) as a flow decomposed into the meridional Ekman drift (given by the zonal wind stress), transporting heat in a shallow surface Ekman layer (o(10m) thick) , and a depth independent compensating return flow, transporting the depth averaged heat content. This is why the Ekman heat transport is most effective if there is a large temperature difference between the shallow surface Ekman layer and below as e.g. in the tropics and the subtropics, whereas if this difference is low, as e.g. in the subpolar regions this contribution is minor. Note, however, that the compensating return flow may not be depth independent, but shallower as in Figure 4. For that case, our definition of the Ekman heat transport will likely overestimate the contribution of the "real" Ekman heat transport. Note also that Ekman heat transport will show up predominantly in the "overturning" part of the heat transport decomposition, since the zonal wind stress has only a weak zonal dependency compared to the meridional one (for both the mean and the NAO–related anomaly).

(not shown). This enhanced heat loss and convection is followed by increasing northward (volume) transport in the upper subpolar gyre and enhanced downwelling north of 45^o N up to lag zero, similar to what was described by Eden and Willebrand (2001) (their Figure 6). However, this developing circulation anomaly in the streamfunction shows no basin-wide pattern. Rather, the anomalous cell is closed a couple of degrees south of 45^o N, which points to enhanced upwelling in the latter region. There is also an obvious signature of the wind stress changes which goes along with a positive or negative NAO in Figure 4. For negative lags, i.e. on average a positive T_a, a shallow negative (positive) cell shows up in the subpolar (subtropical) North Atlantic, in agreement with a southward (northward) wind driven Ekman layer transport in response to anomalous eastward (westward) surface wind stress and a shallow return flow (down to about 500 m).

A similar analysis was done also for HEATONLY. Results are similar, therefore not shown. The major differences compared to STANDARD are first, as expected, the missing shallow Ekman driven flow and, second, small but positive anomalies throughout the North Atlantic for lags -1 to 2 years. The latter is in contrast to STANDARD in which we see a developing small negative anomaly south of 40^o N for the same lags which is, however, replaced by the southward moving large positive anomaly for positive lags. Apparently, this small negative anomaly in STANDARD resembles a lagged (1–2 years) response to changes in the wind stress coming along with the positive T_a. However, the dominant signal in the meridional streamfunction is in both experiments the large positive anomaly developing in response to the enhanced heat loss in the subpolar North Atlantic.

We can now relate this information, to the changes in heat transport by the overturning component in Figure 3. Due to increased upper level northward transport and downwelling for lags of -2 years to about 2 years there is a convergence of heat transport (warming) in the subpolar gyre. For the region south of the intergyre boundary there is a divergence (cooling) due to northward export of heat into the subpolar North Atlantic. The effect on SST is supported by cooling of the upper ocean due to enhanced upwelling of cold water from below. For lags greater than 4 years (not shown) a sequence of opposite sign follows, since at this time the NAOI tends to be negative with reduced heat loss in

the subpolar region and the opposite effect on the meridional circulation, in agreement with Figure 3.

To relate the THC index to changes in the horizontal circulation, Figure 5 shows regression maps of the barotropic streamfunction versus the THC index for STANDARD again for lags from -4 years to 4 years (index leads). We see on average for negative lags, i.e. a positive T_a and increasing strength of the overturning, a positive (anticyclonic) circulation anomaly located at the intergyre boundary at -4 years lag, moving southward up to lag zero and disappearing afterwards. A second, negative (cyclonic) anomaly shows up in the subpolar gyre at around lag -2 years, increasing and moving southward for positive lags. A similar analysis for HEATONLY (not shown), does show this second, negative anomaly, however with reduced amplitude, but lacks the first, positive anomaly. Thus, we can relate this positive anomaly and the enhanced amplitude of the negative anomaly to wind stress changes. The positive (negative), anticyclonic (cyclonic) anomaly at -4 (+3) years lag corresponds to the barotropic oceanic response to a wind stress pattern related to a positive (negative) NAO. The response is obviously given by the topographic Sverdrup response as described by Eden and Willebrand (2001).

How can this circulation change contribute to the gyre heat transport in Figure 3? Heat transport by the horizontal gyres is in general of minor importance in the mid– to high–latitude North Atlantic compared to the contribution of the meridional circulation (Böning et al., 1995) with the exception of the intergyre boundary, and north of it, where the gyre heat transport becomes equally important. Related to the positive gyre anomaly for a positive T_a (-4 year lag) anomalous northward transport of colder (than the zonal average) water at the western boundary and anomalous southward transport of warmer water in the east can be expected. Both are negative contributions to the gyre heat transport, thus warming (cooling) the region south (north) of the intergyre boundary, in agreement with Figure 3. For HEATONLY, the gyre contribution is considerably reduced.

To give now finally a more basinwide picture of the heat transport changes, Figure 6 shows the convergence and divergence of the heat transport related to the THC index, similar to the above figures for STANDARD and HEATONLY. For negative lags up to -1 to -2 years in STANDARD, a warming

(cooling) of the subtropical (subpolar) North Atlantic shows up and for positive lags the influence of the circulation is of opposite sign. The transition occurs around -2 to zero years lag, in agreement to what one would expect from the changes in the meridional circulation. The difference between STANDARD and HEATONLY lies in the reduced amplitude of the warming/cooling, especially the reduced amplitude for negative lags due to the missing positive feedback on T_o due to the changes in the horizontal circulation. Coming back to Figure 1, we can conclude that the reason for the reduced variance and the weaker, more damped oscillation in HEATONLY compared to STANDARD is the positive feedback by the horizontal circulation changes on T_o related to the instantaneous ("topographic–Sverdrup") wind driven response.

These conclusions are further confirmed by comparing SST anomalies from the experiments in relation to the THC index. Figure 7 shows a lagged regression of the annual mean SST against the THC index for STANDARD. Overlaid are also results from a similar regression of the near surface circulation changes. For negative lags, a cold subpolar and a warm subtropical North Atlantic shows up, both giving positive contributions to the SST–index T_o, thus favoring a positive T_a. However, a certain proportion of the amplitudes of the SST anomalies and, accordingly, T_o will be directly induced by the impact of the local surface heat flux changes related to the high value of T_a. To quantify the relative impact of circulation changes and local surface heat fluxes we can utilize experiment HEATONLY.

Figure 8 shows a corresponding analysis for this experiment. Here, only moderate SST anomalies (about half compared to STANDARD) show up for negative lags, supporting the importance of the impact of the changes in the horizontal circulation in STANDARD due to the wind stress changes. Note also that almost no changes in the near surface circulation compared to STANDARD show up for negative lags in HEATONLY. Thus we can relate the near surface circulation anomalies for negative lags in STANDARD to the wind stress forcing. They are maximal near the subpolar front, where these circulation anomalies are northward in the western basin and southward in the east. Note that the zonal gradient in the mean temperature at this depth and latitude is positive, therefore giving rise

to a negative contribution to the gyre heat transport.

For zero lag, SST anomalies in STANDARD as well as in HEATONLY are weak and unstructured such that no large projection onto the SST feedback pattern results. This implies that T_a is unforced by the ocean on average at this time, which is why T_a is about zero at zero lag in Figure 2. For positive lags, the opposite picture develops, but here both for STANDARD and HEATONLY, leading to a tendency for the sign of T_a to change after about 2–4 years. Note that the anomalous upwelling between 40^o and 45^o N developing from -2 to +2 years lag appears to be responsible for the negative SST anomalies for positive lags both in STANDARD and HEATONLY. The warming of the subpolar North Atlantic for positive lags can be related to the increased overturning circulation and northward heat transport.

3 Time scale and damping of the oscillation

Having described the nature of the damped oscillation, we will proceed in this section towards an understanding of the physical mechanism. A key question is what determines the time scale of the oscillation. We focus here on the increase in the overturning since this appears to be an important ingredient of the mechanism from the above discussion. There are two competing hypotheses concerning the mechanism of the onset of the THC anomaly: baroclinic waves and advective processes.

The first could consist of either baroclinic Rossby waves in the interior of the ocean or viscous boundary waves (Davey et al., 1983; Hsieh et al., 1983; Greatbatch and Peterson, 1996). Since the viscous boundary layer associated with these waves is barely resolved in the model, we expect the boundary waves to be very similar to the "numerical" boundary waves discussed by Killworth (1985). The propagation of both Rossby waves and Killworth's boundary waves depends in a similar way on the stratification, i.e. proportional to the square of the gravity wave speed [3], and therefore faster for higher stratification.

[3] For the resolution dependent boundary waves, the propagation speed may be formulated as $c^2/(f\Delta x)$ (Killworth, 1985) where c is the gravity wave speed, and Δx is the model resolution. Note that the dependence is on c^2/f, but not $(c/f)^2$ (which is equal to the square of the Rossby radius) as for long Rossby waves.

In our case, a situation with a high NAO comes along with weaker stratification and vice versa for a low NAO. We have calculated the first mode baroclinic wave speeds for the experiment described by Eden and Jung (2001) (their experiment EXMAIN). Figure 9 shows the mean wave speeds in the North Atlantic and the changes in the wave speed as a composite between a high NAO–phase (1990–1997) minus a phase with persistently low values for the NAOI (1960–1980). In the western subpolar North Atlantic the decrease in wave speeds in this composite is largest, up to 80% of the mean value. Thus, if the onset of the THC anomaly is induced by viscous boundary waves or Rossby waves in this region we would expect a large increase (decrease) in the period of the oscillation at times of a persistently high (low) NAO.

What is the advective time scale in the subpolar North Atlantic? We concentrate here on the abyssal advection out of the convectively active subpolar North Atlantic (mainly the Labrador Sea, cf. Eden and Willebrand (2001)), since advective time scales appear too fast in the upper ocean, with advective pathways rather closed and restricted to the subpolar gyre with no effective export to the subtropics (not shown). We have calculated neutrally buoyant particle trajectories using the mean state of the OGCM, deployed in the convection region in the Labrador Sea, as shown in Figure 10. Almost all particles stayed in the level of upper NADW, in which they were deployed and made their way southwards to the subtropical North Atlantic. As determined from the particles, the advective time scale from the Labrador Sea to about 48^o N is about 3–6 years. Thus, the mean advective time scale is in good agreement with the time scale of the propagation (onset) of the THC anomalies in Figure 4, although it remains unclear to what extent these advective time scales relate to propagation time scales of a density anomaly in the presence of diffusion (although we use isopycnal diffusion in the model with only a small effect on density). Note that in the case of a passive tracer, diffusion will act to shorten the time scale, as e.g. shown by Khatiwala et al. (2001). However, observational estimates of propagation time scales give similar numbers, e.g. Molinari et al. (1997) reported a time scale of about 12 years for an anomaly in newly formed Labrador Sea Water to reach Bermuda (compared to about 15 years in our model, as can be seen from Figure 10).

We expect only moderate changes in the time scale of the damped oscillation due to anomalous advection compared to mean advection or wave processes, since the THC anomalies are typically of the order of 10% in the model. This does not imply that anomalous advection is unimportant. Rather, we are arguing that it is not likely to influence the time scale much if the advective process operates as the dominant mechanism (as it will turn out below, anomalous advection is important to sustain the oscillation). Since a high NAO is followed by increased THC and thus enhanced southward advection of deep density anomalies, a high NAO should lead to a reduced period if advection is important, in contrast to slower wave speeds and a therefore increased period if wave processes are important.

To answer now the question concerning the importance of waves versus advection, we consider here the following set of experiments with the OGCM. We replace the noise term in the simple atmosphere by a positive (experiment NAO+2) or negative (experiment NAO-2) constant which corresponds to a value of the NAOI of $\pm$ 2. We expect the coupled model to respond with a damped oscillation of a certain period. Furthermore, we make use of the semi–prognostic method as proposed by Sheng et al. (2001). The method and its impact on wave speeds and anomalous advection is discussed in Appendix B; here we note two important effects: the propagation speeds of both long, baroclinic Rossby waves and Killworth-type boundary waves, as well as anomalous geostrophic advection are reduced by half with the semi–prognostic approach as used here. It should be noted, that the way we use the semi–prognostic method (see Appendix B for details) the mean state of the model remains unchanged and the effect of mean advection and the barotropic response to wind stress changes are the same as in the prognostic model. Use of the semi–prognostic method should, therefore, help us to unravel the important dynamics (waves versus advection) in the mechanism of our damped oscillation, as we shall show, and we want to propose this method for similar (coupled) model studies. We repeat NAO+2 using the OGCM with the semi–prognostic method (experiment SEMI+2). All experiments start after the 30 year long spin up integration and last for 40 years.

Figure 11 a) shows the time series for T_o for each of the experiments (note that for NAO-2 the negative of T_o is shown). The OGCM shows, as expected, a damped oscillation in all experiments

with, however, slightly different periods and damping time scales. The period in each experiment can be more clearly seen in Figure 11 b), which shows the regression of T_a against the THC index for each experiment in the same manner as Figure 2.

The period in NAO+2 is clearly shorter than in NAO-2, about 12 years in NAO+2 compared to about 16 years in NAO-2. Apparently, the results favor the importance of the advective process, since if wave processes in the western North Atlantic are important, we would expect a longer period in the high NAO case because of the reduced stratification and smaller wave speeds compared with the low NAO case. It seems that the decrease in the period of the oscillation results from the increase of the THC in NAO+2 and the therefore decreased advection time scale. To rule out wave processes, we use SEMI+2, since here, compared to NAO+2, both the anomalous advection *and* wave speeds are reduced everywhere, but the mean advection and the barotropic response to the wind forcing (responsible for the gyre contribution to the heat transport in Figure 3) remains unchanged.

We see in SEMI+2 a strongly damped oscillation with a frequency somewhere in between NAO+2 and NAO-2. From this result we can deduce two things. First, reducing baroclinic wave speeds by half does not seem to effect the period drastically, whereas reducing anomalous geostrophic transports decreases the period with respect to NAO+2 such that it becomes similar to the mean of the periods in NAO+2 and NAO-2. We can conclude that the drastic changes in Rossby and boundary wave speed introduced by the semi-prognostic method have no notable impact on the time scale of the oscillation. Instead, it can be concluded that advection by the mean flow is the dominant factor in setting the (decadal) time scale. In an attempt to enhance the anomalous transport to the value of NAO+2 but still keeping the wave speeds reduced by half, we doubled the anomalous surface heat flux seen by the model, but kept the anomalous wind stress unchanged and repeated SEMI+2 (experiment SEMI++2). Figure 11 b) shows indeed that the period of the damped oscillation in SEMI++2 becomes now more similar to NAO+2. We can conclude that the sum of mean and anomalous geostrophic advection in the subpolar North Atlantic are the important factors controlling the period of the oscillation.

The second conclusion which we draw from the semi–prognostic model is that anomalous geostrophic

transports are sustaining the damped oscillation, since reducing these transports leads to more damping, as can be seen by comparing SEMI+2 with NAO+2. Since it is mandatory to redistribute heat (at least in the surface mixed layer) to effect the SST and therefore the NAO and to sustain a damped oscillation, this change in heat transport can be either triggered by a change in the advected temperature or by a change in the velocities. Therefore, we are also able to conclude that it is the anomalous, geostrophically balanced advection of the mean heat content that is important, not the mean advection of anomalous heat content, in providing the negative feedback part of the oscillation (red curve in Figure 3).

4 Concluding discussion

4.1 Conclusions

We have considered a simple coupled model in which a north–south SST–dipole with its zero line centered along the subpolar front, influences a simple stochastic atmosphere model, taken from Bretherton and Battisti (2000), which in turn forces the OGCM by NAO–related surface heat fluxes and wind stress anomalies. The coupled system exhibits a damped, decadal oscillation. The nature of this oscillation was shown to consist of the following ingredients:

- The OGCM's response to changes in wind stress provides an instantaneous positive feedback by reducing the heat transport across the subpolar front. We found that changes in the oceanic gyre circulation, resulting from the barotropic response to changing wind forcing, are more important than simple Ekman drift changes. Moreover, this immediate response appears to be necessary for a notable damped oscillation, compared to a model without any feedback to the atmosphere in which, nevertheless, a weaker, more strongly damped oscillation can be found as well.

- A negative feedback associated with the baroclinic circulation changes operates on decadal time scale, orchestrated by the onset of an anomaly in the THC located in the subpolar North Atlantic.

This anomaly transports more or less heat across the subpolar front – changing the sign of the SST–dipole, and is related to more or less upwelling in the subtropics.

Using a semi–prognostic model (Sheng et al., 2001), it is possible to reveal the mechanism of the damped oscillation:

- The time scale of the damped oscillation is set by the total advection (the sum of mean and anomalous) out of the subpolar North Atlantic, whereas baroclinic Rossby or boundary waves are unimportant.
- The negative, delayed feedback, necessary to sustain the damped oscillation, is given by the advection of heat by the anomalous, geostrophically balanced currents (and the implied heat transport changes). The advection of anomalous heat by the mean currents (such as "propagating SST anomalies", Sutton and Allen (1997)) is found to be unimportant in sustaining the oscillation in the model.

From the above model results the following picture emerges for the damped oscillation: Clearly, NAO–related surface heat fluxes together with the ocean's response to the wind stress changes generate an SST–dipole pattern which favors an NAOI (T_a) of the same sign and so acts as a positive feedback. At the same time, NAO–related heat loss (gain) in the Labrador Sea generates a deep positive (negative) density anomaly which is advected to the south, generating an east–west pressure gradient favoring enhanced (reduced) southward volume transport in the deep ocean and northward transport in the upper ocean. Since the density anomaly is located at (and north of) the subpolar front, and there is no density anomaly, thus anomalous overturning to the south, we may argue that there must be a compensational upwelling (for an intensified overturning) just south of the deep density anomaly, i.e. between 40 and 45N, where the SST anomalies are strongest (Figure 7 and Figure 8 for lags 2–4y). The upwelling and the heat transport change then acts as a delayed negative feedback to the SST–dipole pattern and thus on the NAO, acting to change its sign on average.

4.2 Discussion

4.2.1 Relationship to other mechanisms

A bundle of thoughts about possible North Atlantic air–sea interactions has been recently proposed by Marshall et al. (2001). Although our model results agree with Marshall et al. (2001) in general terms, we want to stress certain disagreements. In Marshall et al. (2001), a circulation anomaly called the "intergyre–gyre" was proposed to act as a negative feedback on the north–south SST gradient, induced by decadal–scale Rossby wave adjustment to wind stress changes related to the NAO. In the case of a positive NAO, this "intergyre–gyre" was thought to transport more heat northward. In contrast, our model shows this "intergyre–gyre" as the rapid topographic Sverdrup response to the wind stress change. Moreover, in the case of a positive NAO, it *reduces* the heat transport across the subpolar front and acts as a positive feedback on the north–south SST gradient. The negative feedback for the damped oscillation in our model results from the changing THC, proposed by Marshall et al. (2001) as an alternative possibility for a negative feedback. Marshall et al. (2001) might have favored their "intergyre–gyre" scenario, since there is no complete theoretical basis for the description of changes in the THC, in contrast to considerations about baroclinic adjustments of the (flat bottom) wind driven circulation which yield a decadal time scale. Here we have shown that advection of newly formed deep water out of the subpolar North Atlantic sets the (decadal) time scale of the oscillation and that dynamical adjustment processes in the ocean associated with wave processes are of minor importance.

Another interesting idea concerning a possible mechanism of ocean–atmosphere coupling was put forward by Saravanan and McWilliams (1997): "spatial resonance" between advected heat content anomalies in, e.g. the Gulf Stream/North Atlantic Current system, and an overlying stochastic atmosphere (again driven by white, weather noise) might occur on decadal time scales using an appropriate advection time scale in the ocean and a spatially coherent (but temporally white) forcing pattern in the atmosphere. In this setup, ocean dynamics are not needed (only the mean advection) in contrast to e.g. the ideas given by Marshall et al. (2001). A caveat in this model is the surprisingly small

advective velocity that is needed to give decadal scale oscillations; the average, observed speed in the western boundary currents yields a much shorter time scale. Saravanan and McWilliams (1997) argue that it may not be the advective speed in the western boundary current which sets the time scale, but an average, lower speed in a deeper and wider volume around the boundary currents. Similarly, we find in our model "spatial resonance" with an advective time scale, but here, the time scale is set by the deep currents, which easily yields a decadal time scale. In addition, however, changes in ocean currents, induced by the advected deep density anomalies, are necessary for altering the heat transport and therefore the near surface heat content distribution.

4.2.2 How do our results relate to reality?

Häkkinen (1999), Eden and Jung (2001) and Eden and Willebrand (2001) demonstrate that different OGCM's driven by observed forcing variability have skill at simulating the observed time evolution of SST in the North Atlantic on time scales from interannual to interdecadal. Moreover, Eden and Jung (2001) find, in good agreement with observed SST anomalies, that oceanic circulation changes are able to influence mid to high–latitude SST against local atmospheric forcing, as suggested by Bjerknes (1964). But there is less evidence that mid–latitude SST anomalies are effective in influencing the atmosphere. We want to stress that in our model this influence depends crucially on the parameter b of the atmosphere model. A non-zero parameter is supported by the hindcast experiment of, e. g. Rodwell et al. (1999) and the observational studies by Czaja and Frankignoul (2002) and Rodwell and Folland (2002), but this parameter could be small and it remains unclear how effective mid–latitude North Atlantic SST anomalies are in influencing the NAO compared to e.g. tropical Indian/Pacific SST anomalies (Hoerling et al., 2001). On the other hand, Rodwell and Folland (2002) demonstrated recently a potential influence of late winter North Atlantic SST anomalies on the next winter's atmospheric circulation anomalies in the North Atlantic sector based on the analysis of observational data. Studies by Drevillon et al. (2001) and Czaja and Frankignoul (2002) come to similar conclusions. Rodwell and Folland (2002) found, using a linear, multivariate regression analysis, that a

certain North Atlantic SST anomaly in May is related to a mid–troposphere geopotential height (500 hPa) field in a sense of the best linear predictor. The atmospheric signal was found to be similar to NAO–related circulation anomalies. The SST pattern is interestingly akin to what is found in our model: Figure 12 shows regressions between seasonal mean SST anomalies preceding the next winter mean value of T_a. High loadings show up south–east of Newfoundland and in the Irminger Sea with opposite sign. Most significant results and highest values can be found around late spring (A/M/J). During summer time the relation between SST and T_a is apparently lost but shows up again in fall. The pattern and its timing appears to be similar to what is found by Rodwell and Folland (2002). Here we can relate the SST pattern clearly to the changing overturning circulation (compare Figure 12 with Figure 7).

We have shown that it is the mean pathway of recently ventilated water from the Labrador Sea, which orchestrates in the model the onset of the overturning circulation and which sets the delay (in relation to the anomalous forcing) and location of the upwelling at 40N (which has to balance the anomalous overturning further north). A possible concern is that our model might overestimate the advective time scale in the subpolar North Atlantic which sets the frequency of the oscillation, by either too sluggish deep flow due to coarse resolution, or erroneous pathways from the subpolar region to the subtropics.

Molinari et al. (1997) give a time scale of roughly 12 years as an estimate of the propagation speed of a subsurface density anomaly from the Labrador Sea to about 24^o N, which appears slightly shorter than the time scale in our model (about 15 years). On the other hand, a recent study by Rhein et al. (2002) concerning the uptake of anthropogenic trace gases shows that 3 years after a strong convection event (1994) in the Labrador Sea, apparently only about 20% of Labrador Sea Water (LSW) is able to escape the subpolar gyre, which would yield a much longer time scale for such propagation speeds. Using similar observational data, Fine et al. (2002) are able to map ventilation ages on isopycnals, showing smallest "ages" of LSW of 12–14 years at 24^oN and 4–6 years at the subpolar front, thus in good agreement with the time scales in our model.

Another concern is the pathway of the anomalies. The traditional view is that the export of LSW out of the subpolar gyre is concentrated in a Deep Western Boundary Current (DWBC), flowing southward. In contrast, our model shows (Figure 10) the export more in the middle of the basin. This is in agreement with many other ocean models – even high resolution, truly eddy–resolving models agree in this respect with the coarse resolution model version (as the one used in Eden and Böning (2002)) which might support the realism of our model solution. Furthermore, in a recent model study, Yang and Joyce (2003) are able to simulate an eastward swing of the DWBC when it crosses the overlying Gulf Stream (or North Atlantic Current) with a simple reduced gravity model. The reason is the combined effect of the upper current and the sloping continental margin on the lower layer large–scale potential vorticity contours, which gives a reasonable dynamical argument for our model results.

Finally, we want to note the following caveats: First, we concentrate in this study on the mid–latitudes by construction of our model setup and we restrict our conclusion and discussion to this region, without implying anything about the importance of SST–forcing from, e. g. the tropics. And second, while NAO–related changes in evaporation or precipitation appear to be ineffective[4] in forcing the THC, as shown by Eden and Jung (2001), freshwater forcing from other sources, such as changes in freshwater– and ice–export from the Arctic or changes in river runoff related to the NAO may impact the THC in a way not accounted for by our model setup.

Appendix A: Model and coupling strategy

We use the following experimental strategy: first we spin up the OGCM for 30 years using monthly varying surface forcing, which is given by a Barnier–type heat flux formulation (Barnier et al., 1995) and a restoring condition for salinity. The OGCM is part of the FLAME hierarchy of models (see

[4] This is since the freshwater flux pattern which comes along with the NAO shows highest loadings in the eastern North Atlantic, a region in which the THC appears to be less sensitive to surface density fluxes than in the west, where the deep water masses are ventilated. Furthermore, its relative contribution to the surface density fluxes compared to the heat fluxes is minor.

also *http://www.ifm.uni-kiel.de/fb/fb1/tm/research/FLAME/index.html*), the horizontal resolution is $4/3^o \cos\phi$ (ϕ denoting latitude) with 45 vertical levels, and the model domain is the Atlantic from 20^o S to 70^o N. Although the current model version is quite similar to the version used in Eden et al. (2002), some modifications have been introduced: a bottom boundary layer parameterization following Beckmann and Döscher (1997), a third order tracer advection scheme (Quicker) replacing the traditional second order scheme (see Griffies et al. (2000) for the benefits) and a closure for the vertical turbulent kinetic energy following Gaspar et al. (1990) (utilizing identical parameters for the scheme as in Oschlies and Garçon (1998), see also a description of the model improvement therein) replacing a scheme proposed by Gargett (1984). All modifications lead in several ways to an improvement of the mean circulation and tracer distribution in the model. However, their effects on the variability appear to be of minor importance. Note that we have also restricted the model domain to the region north of 20^o S, applying open boundary formulations following Stevens (1990) at 20^o S. More details about the OGCM (except for the mentioned modifications) can be found in Eden and Willebrand (2001).

After the spin-up, the OGCM is coupled to the BB atmosphere model: Monthly varying spatial patterns are multiplied by the NAOI (T_a) from the atmosphere model and the OGCM is forced with the resulting anomalous surface fluxes which are added to the seasonally varying surface flux formulation used in the spin-up. The forcing patterns are derived from a regression of wind stress and heat flux from the NCEP/NCAR reanalysis data (Kalnay et al., 1996) against the observed NAOI [5], as in Eden and Jung (2001) and Eden and Willebrand (2001). The OGCM will eventually produce SST anomalies (relative to the end of the spin-up period), which are projected on to a fixed SST pattern (hereafter referred to as the SST feedback pattern). We identify this projection (now a univariate variable) with the oceanic variable T_o, which is then used to force the simple atmosphere model. Thus we get T_a for the next time step, using bT_o. The atmospheric parameter values and the time stepping for the coupling (5 days) are the same as in Bretherton and Battisti (2000). The SST feedback pattern used

[5] The difference of normalized sea level pressure between Ponta Delgada, Azores and Stykkisholmur–Reykjavik, Iceland.

for the projection of the OGCM's SST anomalies is derived from a regression of the historical record of SST (Smith et al., 1996) against the observed NAOI. We excluded regions in which observations are sparse, e.g. ice covered regions, and regions which we regard as not effective for forcing the atmospheric baroclinicity, such as the loadings in the North Sea. We have also excluded any loadings south of 30^oN, in order to concentrate on mid–latitude SST forcing, while not wishing to imply that in reality, tropical SST forcing may not play a role (although the loadings in the tropics are quite small). Figure 13 shows the original SST regression and the SST feedback pattern we use.

Finally, we need two scaling parameters: one to relate T_o in the BB model and the projection of SST anomalies onto the SST feedback pattern and the second to relate T_a of the BB model with the NAOI. For the first parameter (f_o), we scale T_{ogcm} (the "raw" projection of the SST anomalies to the SST feedback pattern) such that $Var(T_o) = Var(T_{ogcm} f_o)$. We have calculated $Var(T_o)$ analytically from the BB model and estimated $Var(T_{ogcm})$ from a previous hindcast model experiments over the last 40 years (Eden and Jung, 2001). For the second parameter, we scale T_a with f_a such that $Var(T_a f_a) = Var(NAO)$. We took $Var(NAO)$ from observations and $Var(T_a)$ analytically from the BB model, which gives a value of $f_a = 4.56$ [6]. All experiments discussed in this study are driven with the same realization of white noise. This white noise has been generated with MATLAB using the command "normrnd" with zero mean and unit variance after initializing the program.

Note that we account for the damping influence of the model's surface heat flux boundary condition by using $Var(T_{ogcm})$ from a model experiment instead of using observed SST anomalies. If we would use the "observed" variance of T_{ogcm} to calculate the scaling parameter f_o, there would be an spurious effect on the coupling strength, i.e a different "effective" b than set in the BB model. Using the "modeled" variance of T_{ogcm} on the other hand yields, in our view, the correct scaling parameter, the correct "effective" parameter b and the correct relative influence of heat flux versus wind stress forcing on SST–anomalies.

[6] Note, that it is necessary to compare variances on the 5–day time scale for the atmospheric case, while for the oceanic variables this caveat is of minor importance. We have assumed that a third of the total variance for the NAOI, (as it is approximately the case for T_a in the BB model) is contained in a band between 5–day and monthly periods

Appendix B: The semi–prognostic method as a diagnostic tool

Conventionally, a diagnostic model is an OGCM in which potential temperature and salinity are held fixed at certain climatological values and in which the momentum remains as the only prognostic variable. There are certain disadvantages involved with such an approach, as discussed by, e.g. Greatbatch et al. (1991). Due to small discrepancies between the prescribed baroclinic structure and the discretized model topography large, spurious currents can occur since the density structure cannot be adjusted as in a freely evolving prognostic model. In an attempt to overcome this problem, model density is sometimes relaxed towards a climatology on a short time scale of order of days ("nudging"), which is then called a robust diagnostic model (Sarmiento and Bryan, 1982). However, it is obvious that unphysical sources and sinks of heat and salt are introduced by such an approach. Sheng et al. (2001) proposed a method to adiabatically change the advection properties of a hydrostatic OGCM by altering the pressure gradient seen by the model in the momentum balance. The (baroclinic) pressure gradient used in the model's momentum equation is obtained by vertical integrating a linear combination of the gradient of the model density and of a certain specified density, e.g. climatology. Using the model density only yields a conventional, prognostic model, using the specified density only yields a diagnostic model and using a combination of both (here taken as half and half) yields a semi–prognostic model. The method can be viewed as a simple data assimilation technique, with the advantage over other simple methods, e.g. "nudging", that no spurious diabatic sources and sinks are introduced. Sheng et al. (2001) applied the method with good success to a regional model of the north–western Atlantic.

Since velocity is approximately in geostrophic balance in the ocean, it is obvious that a semi–prognostic model will under-represent anomalous velocities, induced by either internal instability processes, i.e. eddies, or surface forcing variability, depending on the amount by which model density or specified density is used for the calculation of the pressure gradient. For the same reason, geostrophic waves like, Rossby waves and viscous boundary waves, are influenced such that wave speeds are de-

creased by a similar amount (inviscid, baroclinic Kelvin wave speeds are reduced by the square root of the proportionality constant).

It should be noted, that this somehow spurious behavior of the semi–prognostic method (including its damping effect on eddy activity) can be eliminated by diagnosing the correction applied by the (flow–interactive) method from a spin-up integration and by applying a corresponding fixed (non flow–interactive) correction in a subsequent integration. The authors will discuss such methods in a separate manuscript (Eden, Greatbatch and Böning, 2002, submitted to JPO).

However, here we want to make use of the damping effect of the semi–prognostic method to explore the possible role of waves versus advection in the mechanism of the damped oscillation described above. After the spin-up, we have applied the semi–prognostic method using the monthly mean *model* density as the specified density, instead of density taken from observations as in Sheng et al. (2001). A subsequent 10 year integration (with no change in the surface forcing) reveals almost no change in the OGCM, except for a small influence on the seasonality in low latitudes. Since the method changes baroclinic wave propagation speeds and anomalous geostrophic advection, it can be used, as we show in Section 3, as a tool to diagnose the relative importance of different dynamical processes. An advantage of this method, compared to e.g. acceleration techniques (Bryan, 1984), is that it does not effect advection by the mean flow nor barotropic processes. We consider this method to be very powerful and want to promote it in studies concerning variability in the ocean and as well as in the atmosphere.

Acknowledgments

This work has been supported by funding provided to the Canadian CLIVAR Research Network by NSERC, CFCAS and CICS. We are also grateful for the use of computer facilities of the Canadian Meteorological Centre in Dorval, Quebec, Canada.

References

Barnier, B., L. Siefridt, and P. Marchesiello, 1995: Thermal forcing for a global ocean circulation model using a three year climatology of ECMWF analysis. *J. Mar. Sys.*, **6**, 363–380.

Beckmann, A. and R. Döscher, 1997: A method for improved representation of dense water spreading over topography in geopotential-coordinate models. *J. Phys. Oceanogr.*, **27**, 581–591.

Beismann, J. O., C. W. Böning, and D. Stammer, 2002: Interannual to decadal variability of the meridional overturning circulation of the Atlantic: A comparison of the response to atmospheric fluctuations in three ocean models. Clivar Exchanges.

Bjerknes, J., 1964: Atlantic air sea interaction. *Adv. Geophys.*, **10**, 1–82.

Böning, C. W., W. R. Holland, F. O. Bryan, G. Danabasoglu, and J. C. McWilliams, 1995: An overlooked problem in model simulations of the thermohaline circulation and heat transport in the Atlantic ocean. *J. Climate*, **8**, 515–523.

Bretherton, C. S. and D. S. Battisti, 2000: An interpretation of the results from atmospheric general circulation models forced by the time history of the observed sea surface temperature distribution. *Geophys. Res. Letters*, **27**(6), 767–770.

Bryan, K., 1962: Measurements of meridional heat transport by ocean currents. *J. Geophys. Res.*, **67**, 3403–3414.

Bryan, K., 1984: Accelerating the convergence to equilibrium of ocean–climate models. *J. Phys. Oceanogr.*, **14**, 666–673.

Cassou, C. and L. Terray, 2001: Dual influence of Atlantic and Pacific SST anomalies on the Narth Atlantic/Europe winter climate. *Geophys. Res. Letters*, **28**(16), 3195–3198.

Czaja, A. and C. Frankignoul, 2002: Observed impact of Atlantic SST anomalies on the North Atlantic Oscillation. *J. Climate*, **15**(6), 606–623.

Davey, M. K., W. W. Hsieh, and R. C. Wajsowicz, 1983: The free Kelvin wave with lateral and horizontal viscosity. *J. Phys. Oceanogr.*, **12**(12), 2182–2191.

Dewar, W. K., 2001: On ocean dynamics in mid-latitude climate. *J. Climate*, **14**, 4380–4397.

Döscher, R., C. W. Böning, and P. Herrmann, 1994: Response of circulation and heat transport in the North Atlantic to changes in thermohaline forcing in northern latitudes: A model study. *J. Phys. Oceanogr.*, **24**, 2306–2320.

Drevillon, M., L. Terray, P. Rogel, and C. Cassou, 2001: Midlatitude Atlantic SST influence on European winter climate variability in the NCEP reanalysis. *Climate Dyn.*, **18**, 331–344.

Eden, C. and C. W. Böning, 2002: Sources of eddy kinetic energy in the Labrador Sea. *J. Phys. Oceanogr.*, **32**(12), 3346–3363.

Eden, C., R. J. Greatbatch, and J. Lu, 2002: Prospects for decadal prediction of the North Atlantic Oscillation (NAO). *Geophys. Res. Letters*. In press.

Eden, C. and T. Jung, 2001: North Atlantic interdecadal variability: oceanic response to the North Atlantic oscillation (1865–1997). *J. Climate*, **14**(5), 676–691.

Eden, C. and J. Willebrand, 2001: Mechanism of interannual to decadal variability of the North Atlantic circulation. *J. Climate*, **14**(10), 2266–2280.

Fine, R., M. Rhein, and C. Andrie, 2002: Using a CFC effective age to estimate propagation and storage of climate anomalies in the deep western North Atlantic Ocean. *Geophys. Res. Letters*, **29**(24), 80–1–80–4.

Gargett, A. E., 1984: Vertical eddy diffusivity in the ocean interior. *J. Mar. Res.*, **42**, 359–393.

Gaspar, P., Y. Gregoris, and J.-M. Lefevre, 1990: A simple eddy kinetic energy model for simulations of the oceanic vertical mixing: tests at station PAPA and Long-Term Upper Ocean Study site. *J. Geophys. Res.*, **95**, 16179–16193.

Gerdes, R. and C. Köberle, 1995: On the influence of DSOW in a numerical model of the North Atlantic general circulation. *J. Phys. Oceanogr.*, **25**(11), 2624–2642.

Goodman, P. J., 2001: Thermohaline adjustment and advection in an OGCM. *J. Phys. Oceanogr.*, **31**(6), 1477–1497.

Greatbatch, R. J., 2000: The North Atlantic Oscillation. *Stochastic Enviromental Research and Risk Assessment*, **14**, 213–241.

Greatbatch, R. J., A. F. Fanning, A. D. Goulding, and S.Levitus, 1991: A diagnosis of interpentadal circulation changes in the North Atlantic. *J. Geophys. Res.*, **96**, 22009–22023.

Greatbatch, R. J. and K. A. Peterson, 1996: Interdecadal variability and oceanic thermohaline adjustment. *J. Geophys. Res.*, **101**(C9), 20467–20482.

Griffies, S. M., R. C. Pacanowski, and B. R. Hallberg, 2000: Spurious diapycnal mixing associated with advection in a z-coordinate ocean model. *Mon. Wea. Rev.*, **128**, 538–564.

Gulev, S. K., B. Barnier, H. Knochel, J. M. Molines, and M. Gottet, 2003: Water mass transformation in the North Atlantic and its impact on the meridional circulation: insights from an ocean model forced by NCEP/NCAR reanalysis surface fluxes. Submitted to J. Clim.

Häkkinen, S., 1999: Variability of the simulated meridional heat transport in the North Atlantic for the period 1951–1993. *J. Geophys. Res.*, **104**(C5), 10991–11007.

Häkkinen, S., 2001: Variability in sea surface height: a qualitative measure for the meridional overturning in the north atlantic. *J. Geophys. Res.*, **106**(C7), 13837–13848.

Hoerling, M., J. W. Hurrell, and T. Xu, 2001: Tropical origins for recent North Atlantic climate change. *Science*, **292**, 90–92.

Hsieh, W. W., M. K. Davey, and R. C. Wajsowicz, 1983: The free Kelvin wave in finite–difference numerical models. *J. Phys. Oceanogr.*, **13**(8), 1383–1397.

Hurrell, J. W., 1996: Influence of variations in extratropical wintertime teleconnections on Northern Hemisphere temperature. *Geophys. Res. Letters*, **23**, 665–668.

Johnson, H. L. and D. P. Marshall, 2002: A theory of the surface Atlantic response to thermohaline variability. *J. Phys. Oceanogr.*, **32**, 1121–1132.

Kalnay, E., M. Kanamitsu, R. Kistler, W. Collins, D. Deaven, L. Gandin, M. Iredell, S. Saha, G. White, J. Woollen, Y. Zhu, M. Chelliah, W. Ebiszusaki, W. Higgins, J. Janowiak, K. Mo, C. Ropelewski, J. Wang, A. Leetmaa, R. Reynolds, R. Jenne, and D. Joseph, 1996: The NCEP/NCAR 40-years renanalysis project. *Bull. Amer. Meteor. Soc.*, **77**, 437–471.

Khatiwala, S., M. Visbeck, and P. Schlosser, 2001: Age tracers in an ocean GCM. *Deep-Sea Res.*, **48**, 1423–1441.

Killworth, P. D., 1985: A two level wind and buoyancy–driven thermocline model. *J. Phys. Oceanogr.*, **15**, 1414–1432.

Kushnir, Y., 1999: Europe's winter prospects. *Nature*, **398**, 289–291.

Latif, M., K. Arpe, and E. Röckner, 2000: Oceanic control of decadal North Atlantic sea level pressure variability in winter. *Geophys. Res. Letters*, **27**, 727–730.

Lu, J. and R. J. Greatbatch, 2002: The changing relationship between NAO and northern hemisphere climate variability. *Geophys. Res. Letters*, **29**(7), 52–1–52–4.

Marotzke, J. and B. A. Klinger, 2000: The dynamics of equatorially asymmetric thermohaline circulations. *J. Phys. Oceanogr.*, **30**(5), 955–970.

Marshall, J., H. Johnson, and J. Goodman, 2001: A study of the interaction of the North Atlantic Oscillation with ocean circulation. *J. Climate*, **14**, 1399–1421.

Mehta, V. M., M. J. Suarez, J. Manganello, and T. L. Delworth, 2000: Oceanic influence on the North Atlantic Oscillation and associated northern hemisphere climate variations. *Geophys. Res. Letters*, **27**, 121–124.

Molinari, L. R., D. A. Mayer, J. F. Festa, and H. F. Bezdek, 1997: Multiyear variability in the near-surface temperature structure of the midlatitude western North Atlantic Ocean. *J. Geophys. Res.*, **102**(C2), 3267–3278.

Molteni, F. and S. Corti, 1998: Long–term fluctuations in the statistical properties of low–frequency variability: dynamical origin and predictability. *Quart. J. Royal Met. Soc.*, **124**, 495–526.

Oschlies, A. and V. Garçon, 1998: Eddy induced enhancement of primary production in a model of the North Atlantic Ocean. *Nature*, **394**, 266–269.

Peterson, K. A., R. J. Greatbatch, J. Lu, H. Lin, and J. Derome, 2002: Hindcasting the NAO using diabatic forcing of a simple AGCM. *Geophys. Res. Letters*, **29**(9), 10.1029/2001GL014502.

Rhein, M., J. Fischer, W. M. Smethie, D. Smythe-Wright, R. F. Weiss, C. Mertens, D. H. Min, U. Fleischmann, and A. Putzka, 2002: Labrador Sea Water: Pathways, CFC-inventory, and formation rates. *J. Phys. Oceanogr.*, **32**, 648–665.

Robertson, A. W., C. R. Mechoso, and Y.-J. Kim, 2000: The influence of Atlantic Sea Surface Temperature anomalies on the North Atlantic Oscillation. *J. Climate*, **13**, 122–138.

Rodwell, M. and C. K. Folland, 2002: Atlantic air–sea interaction and seasonal predictability. *Quart. J. Royal Met. Soc.*. In press.

Rodwell, M., D. P. Rowell, and C. K. Folland, 1999: Oceanic forcing of the wintertime North Atlantic Oscillation and European climate. *Nature*, **398**, 320–323.

Saravanan, R. and J. C. McWilliams, 1997: Stochasticity and spatial resonance in interdecadal climate fluctuations. *J. Climate*, **10**, 2299–2320.

Sarmiento, J. L. and K. Bryan, 1982: An ocean transport model for the North Atlantic. *J. Geophys. Res.*, **87**, 394–408.

Sheng, J., R. J. Greatbatch, and D. Wright, 2001: Improving the utility of ocean circulation models through adjustment of the momentum balance. *J. Geophys. Res.*, **106**, 16711–16728.

Smith, T. M., R. E. Reynolds, R. E. Livezey, and D. C. Stokes, 1996: Reconstruction of Historical Sea Surface Temperatures using Empirical Orthogonal Functions. *J. Climate*, **9**, 1403–1420.

Stevens, D. P., 1990: On open boundary conditions for three dimensional primitiv equation ocean circulation models. *Geophys. Astrophys. Fluid Dyn.*, **51**, 103–133.

Sutton, R. T. and M. R. Allen, 1997: Decadal predictability of North Atlantic sea surface temperature and climate. *Nature*, **388**, 563–567.

Wallace, J. M. and D. S. Gutzler, 1981: Teleconnections in the geopotential height field during the northern hemisphere winter. *Mon. Wea. Rev.*, **109**, 784–812.

Yang, J. and T. M. Joyce, 2003: How do high–latitude North Atlantic climate signals crossover between the Deep Western Boundary Current and the Gulf Stream. *Geophys. Res. Letters*, **30**(2), 42–1–42–4.

Figure captions

Fig. 1 **Upper panel:** Annual means of T_a (scaled NAOI) from STANDARD (blue line), HEATONLY (red) and UNCOUPLED (green).

Lower panel: Same as upper panel but T_o (SST–index).

Fig. 2 **Left panel:** Regression of annual means of T_a taken from STANDARD against the overturning (THC) index at different lags (atmosphere leads for negative lags). See text for the definition of the THC index. Filled circles denote significant regression slopes disregarding a null hypothesis (uncorrelated white noise) at the 95% level.

Right panel: Same as left panel but for HEATONLY.

Fig. 3 Lagged regression of annual means of heat transport (and decompositions) at 48^{o}N taken from STANDARD against the THC index (index leads for positive lags). The thick solid line denotes total advective heat transport (PW/Sv), the dotted line the "overturning" component, dashed the "gyre" component and the thin solid Ekman heat transport. The standard deviation of the THC index in STANDARD is 0.98 Sv.

Fig. 4 Regression of annual means of the meridional streamfunction in STANDARD against the THC index at different lags (lags are denoted in the figures, index is leading for positive lags). Contour interval is 0.1. Shaded regions (light grey) share significant (95% level) slopes.

Fig. 5 Regression of annual means of the horizontal streamfunction taken from STANDARD against the THC index at different lags (as denoted in the figures, index is leading for positive lags). Contour interval is 0.25 Sv/Sv. Values range from -2.5 Sv/Sv to 2.5 Sv/Sv. Shaded regions (light grey) share significant (95% level) slopes. The standard deviation of the THC index in STANDARD is 0.98 Sv.

Fig. 6 **Left panel:** Regression of annual mean northward heat transport convergence taken from STANDARD against the THC index as a function of latitude and lag (index leads for positive

lags). Positive slopes denote warming of the ocean for positive anomalies of the THC index. Contour interval is 10 $GW/m/Sv$ and grey-shaded are regions with significant slopes at a 95% level. The standard deviation of the THC index in STANDARD is 0.98 Sv.

Right panel: Same as left panel but for HEATONLY. The standard deviation of the THC index in HEATONLY is 0.49 Sv.

Fig. 7 Regression of annual means of SST and velocity at $100m$ depth taken from STANDARD against the THC index at different lags (as denoted in the figures, index is leading for positive lags). Shading ranges from -0.36 K/Sv to 0.36 K/Sv for SST, the units for velocity are $cm/s/Sv$. SST and arrows are shown for regions with significant (95% level) slopes only. A cutoff value of 0.5 $cm/s/Sv$ for velocity is used; a 3-point Hanning window was applied to all fields prior to plotting. Note that the standard deviation of the THC index in STANDARD is 0.98 Sv.

Fig. 8 Same as Figure 7 but for HEATONLY. Note that the standard deviation of the THC index in HEATONLY is 0.49 Sv.

Fig. 9 **Left panel**: The long term mean of the first baroclinic mode Rossby wave speed in $cm\ s^{-1}$ from experiment EXMAIN of Eden and Jung (2001). Wave speeds are calculated by solving the vertical (flat–bottom) eigenvalue problem using the local profile of the annual mean stratification at each grid point and for each year (133y) of the integration. Contour interval is 0.2 mm/s between 0 and 0.2 cm/s, 0.2 cm/s between 0.2 and 2 cm/s and 1 cm/s for larger values.

Right panel: Changes in Rossby wave speeds (in percent) in that experiment as a composite of the 1990's (high NAO) minus the period from 1960 to 1980 (low NAO).

Fig. 10 Trajectories of neutrally buoyant particles advected in the OGCM. Black crosses denotes the deployment region ($\sim$ 1500 m depth); different colors of the trajectories denote 3 year periods.

Fig. 11 **a)** T_o from experiments NAO+2 (blue), NAO-2 (green) and SEMI+2 (red). Note that T_o from NAO-2 was multiplied by minus one to enhance readability.

b) Regression of annual means of T_a against the THC index at different lags (atmosphere leads

for negative lags). Shown are results for the same experiments as in a) using the same color code. Also shown are results from SEMI++2 (dashed red line and crosses).

Fig. 12 **a)** Regression of J/F/M seasonal mean SST against the next winter (J/F/M) value of T_a.

b) to c) same but regression of A/M/J, J/A/S and O/N/D seasonal mean SST against next winter T_a respectively. Contour interval is 0.1 K, grey shading denotes significant regression slope (95% level).

Fig. 13 **Left panel:** Regression of observed SST anomalies versus the observed NAOI. Contour interval is 0.05 K.

Right panel: Resulting SST feedback pattern.

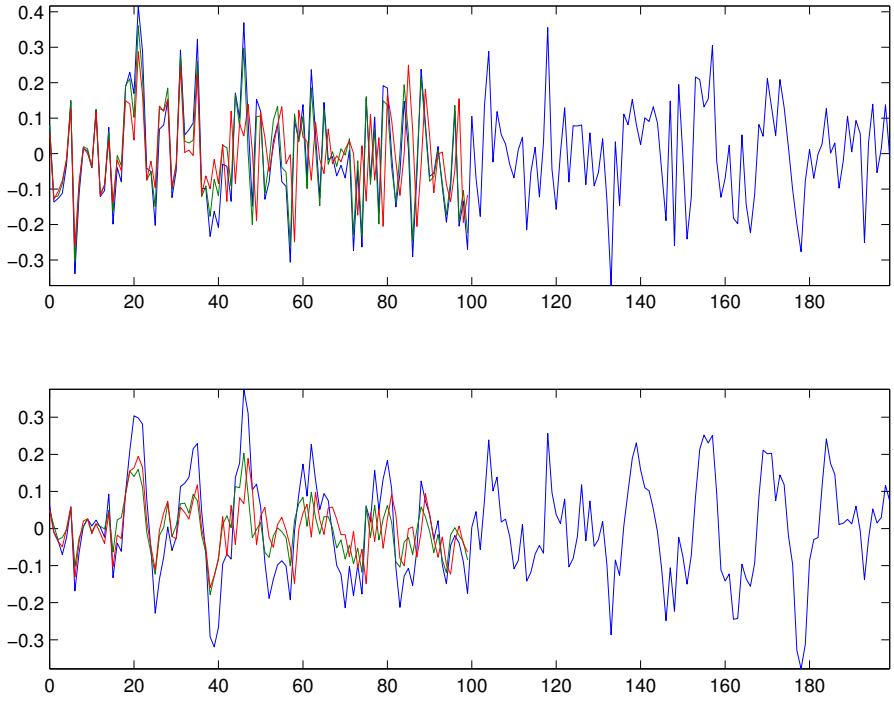
0.4
0.3
0.2
0.1
0
−0.1
−0.2
−0.3
0
20
40
60
80
100
120
140
160
180
0.3
0.2
0.1
0
−0.1
−0.2
−0.3
0
20
40
60
80
100
120
140
160
180

Figure 1:

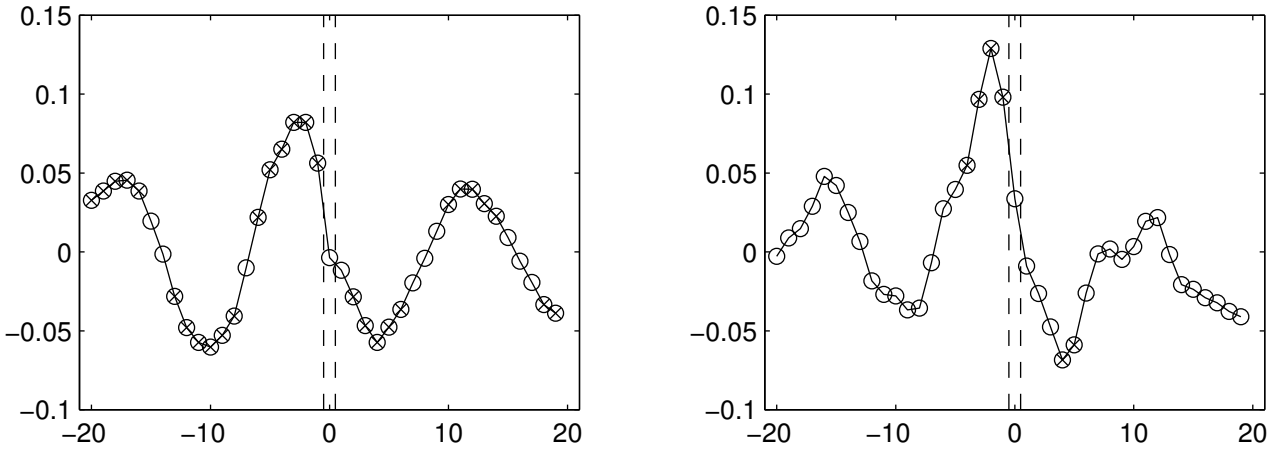

Figure 2:

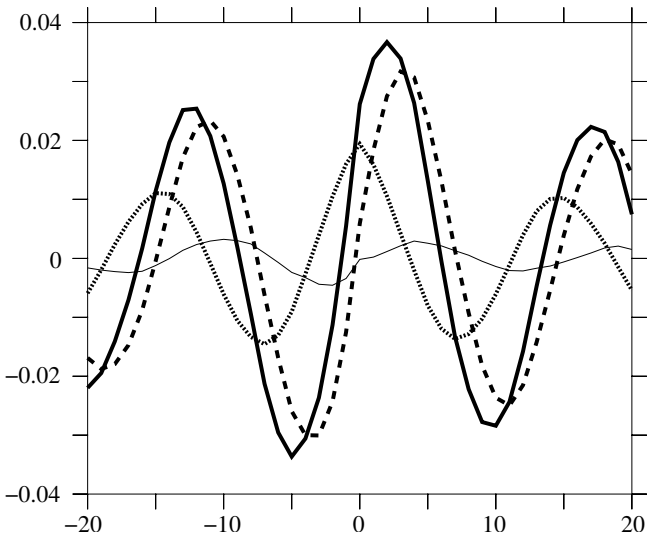

Figure 3:

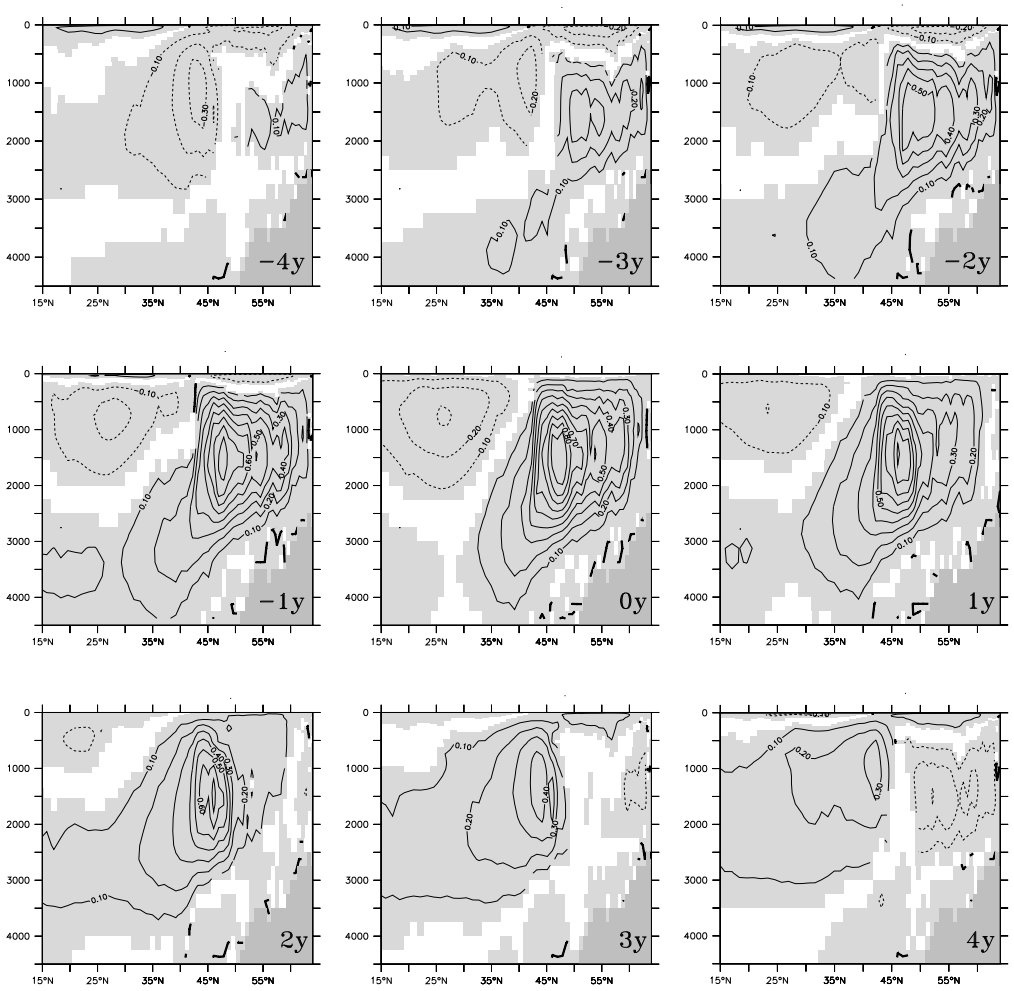
−4y
−3y
−2y
−1y
0y
1y
2y
3y
4y
15°N
25°N
35°N
45°N
55°N
0
1000
2000
3000
4000

Figure 4:

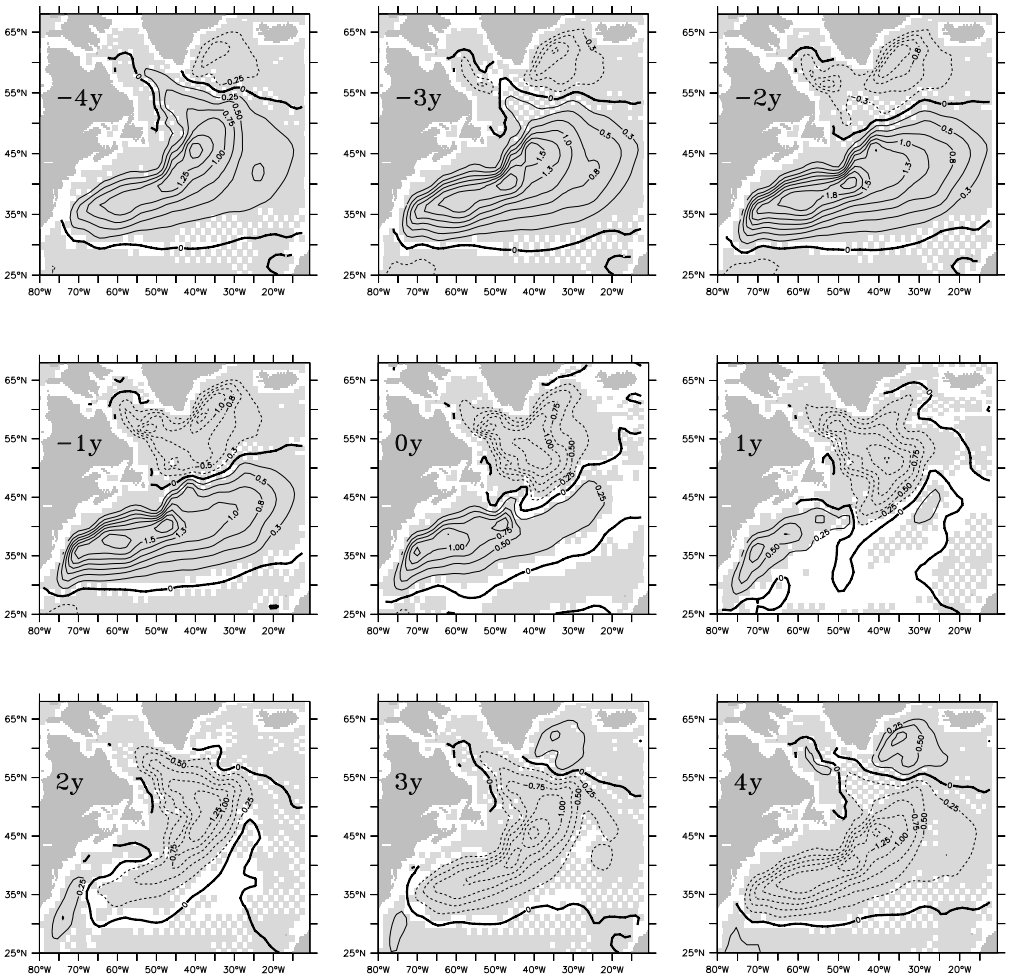
−4y
−3y
−2y
−1y
0y
1y
2y
3y
4y
65°N
55°N
45°N
35°N
25°N
80°W
70°W
60°W
50°W
40°W
30°W
20°W

Figure 5:

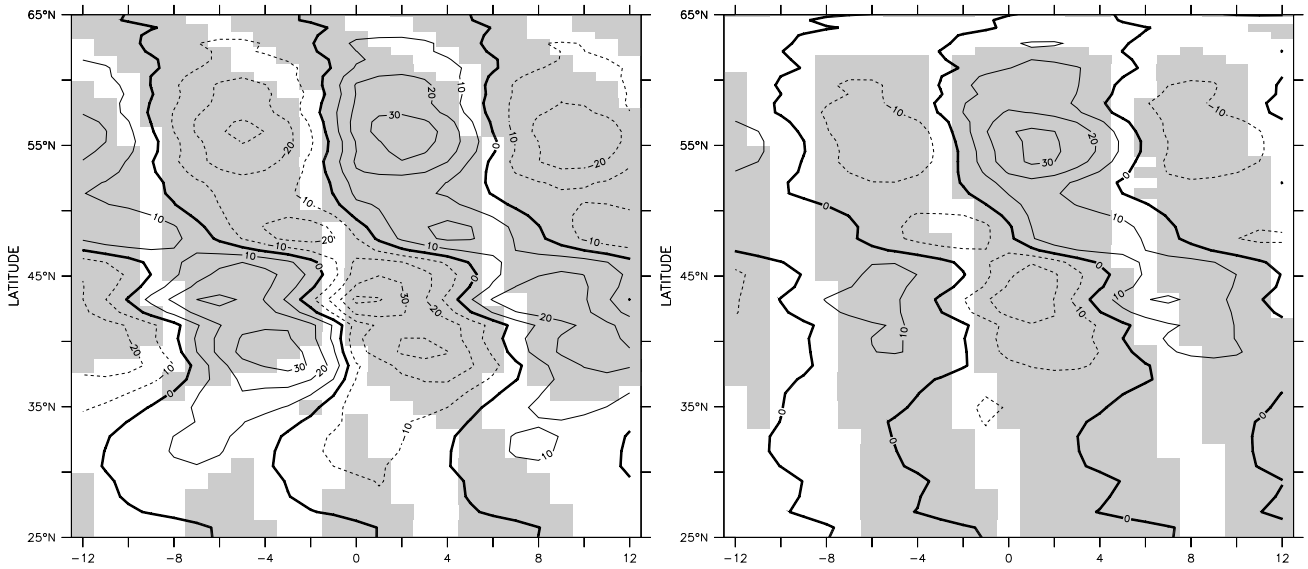

Figure 6:

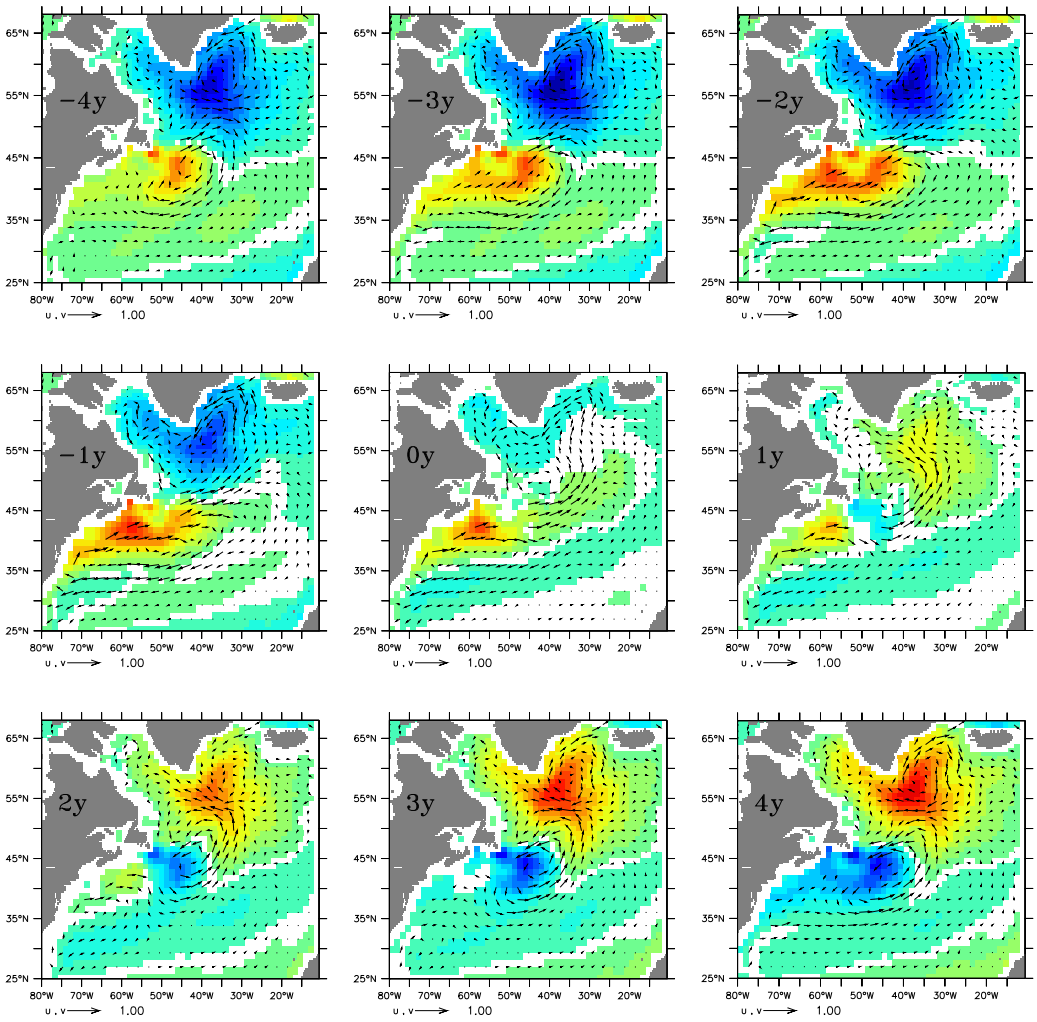
−4y
−3y
−2y
−1y
0y
1y
2y
3y
4y
65°N
55°N
45°N
35°N
25°N
80°W 70°W 60°W 50°W 40°W 30°W 20°W
u , v 1.00

Figure 7:

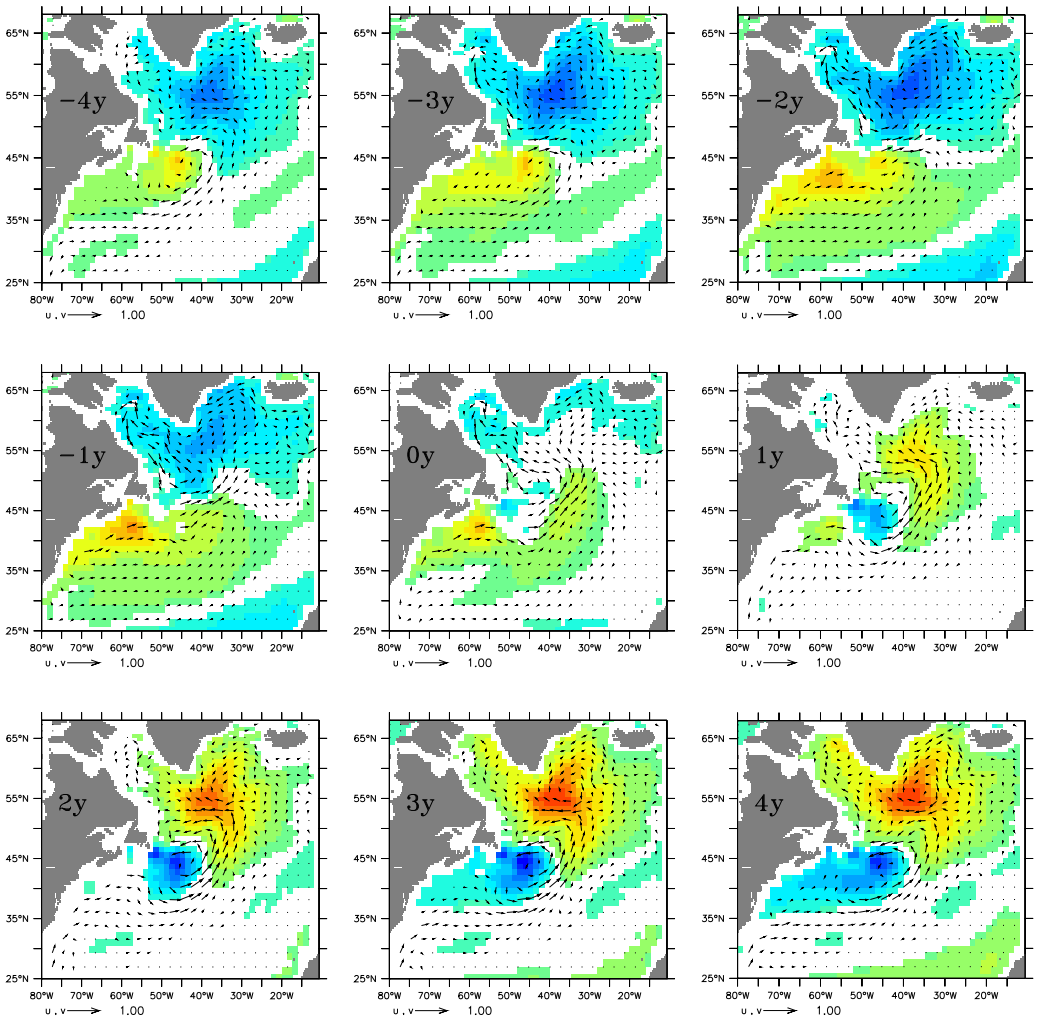
−4y
−3y
−2y
−1y
0y
1y
2y
3y
4y
65°N
55°N
45°N
35°N
25°N
80°W 70°W 60°W 50°W 40°W 30°W 20°W
u , v 1.00

Figure 8:

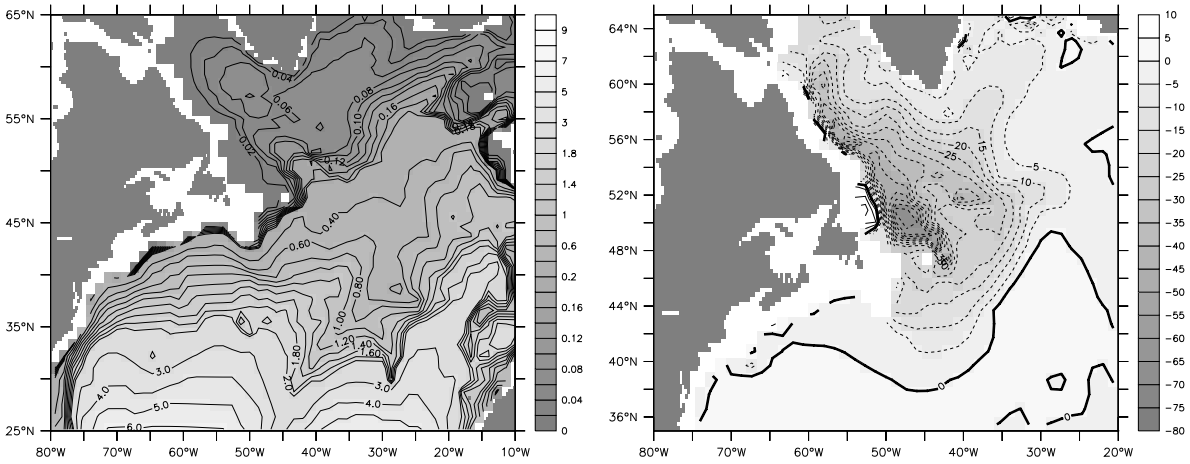
65°N
55°N
45°N
35°N
25°N
80°W
70°W
60°W
50°W
40°W
30°W
20°W
10°W
64°N
60°N
56°N
52°N
48°N
44°N
40°N
36°N
80°W
70°W
60°W
50°W
40°W
30°W
20°W

Figure 9:

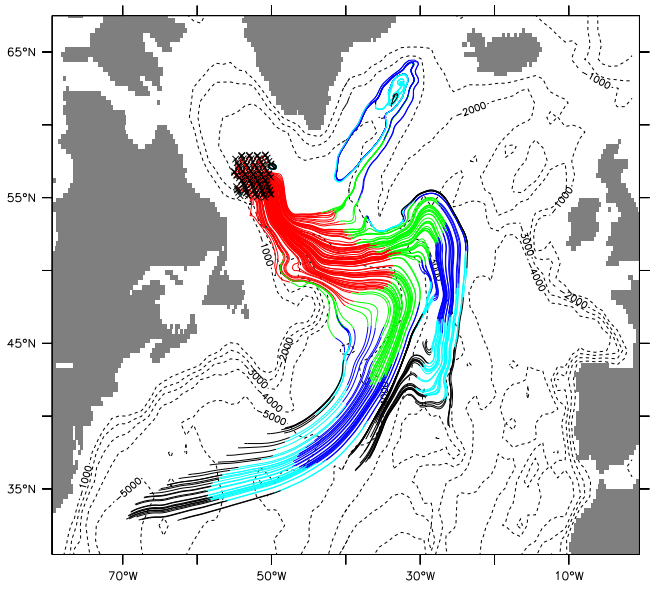

Figure 10:

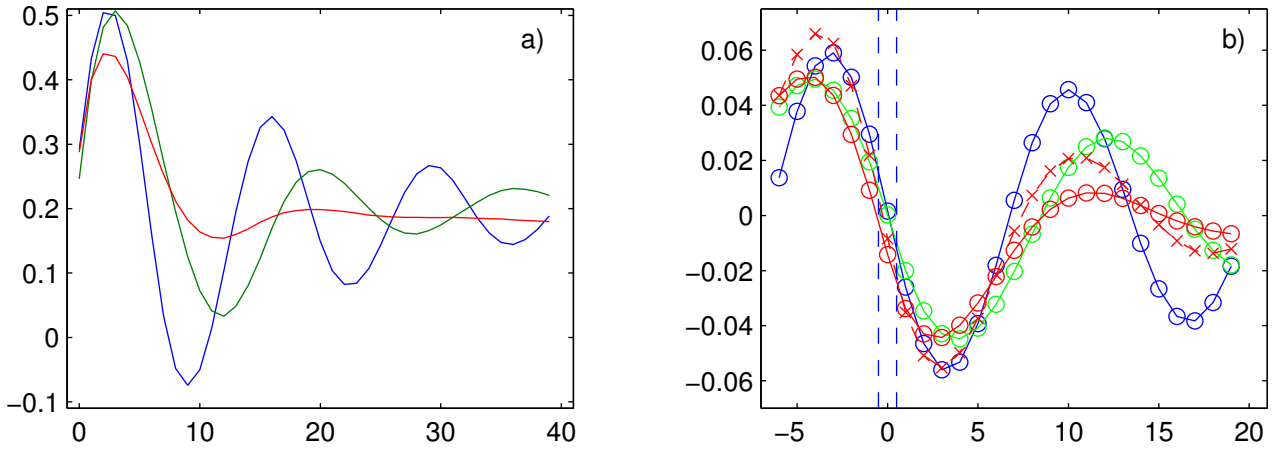
a)
b)
0.5
0.4
0.3
0.2
0.1
0
−0.1
0
10
20
30
40
0.06
0.04
0.02
0
−0.02
−0.04
−0.06
−5
0
5
10
15
20

Figure 11:

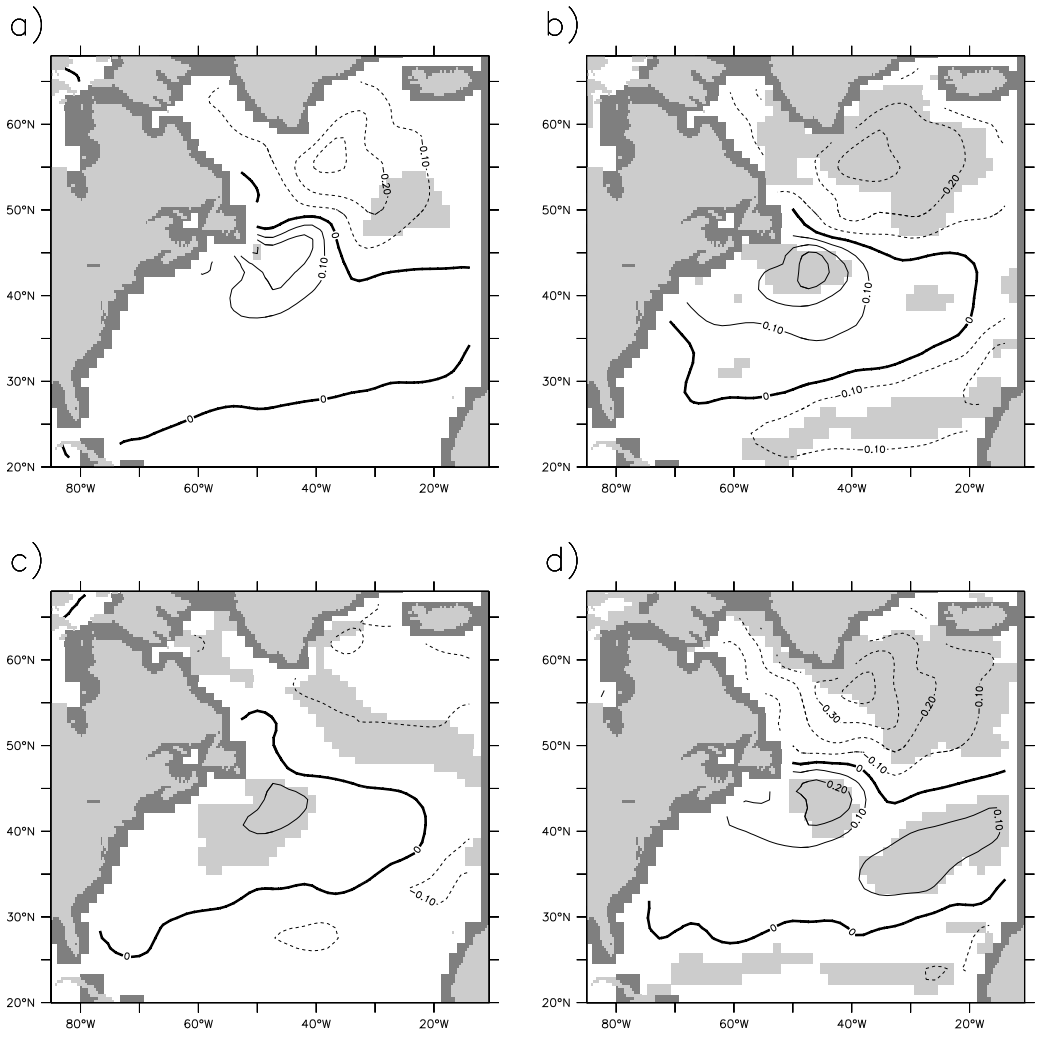

Figure 12:

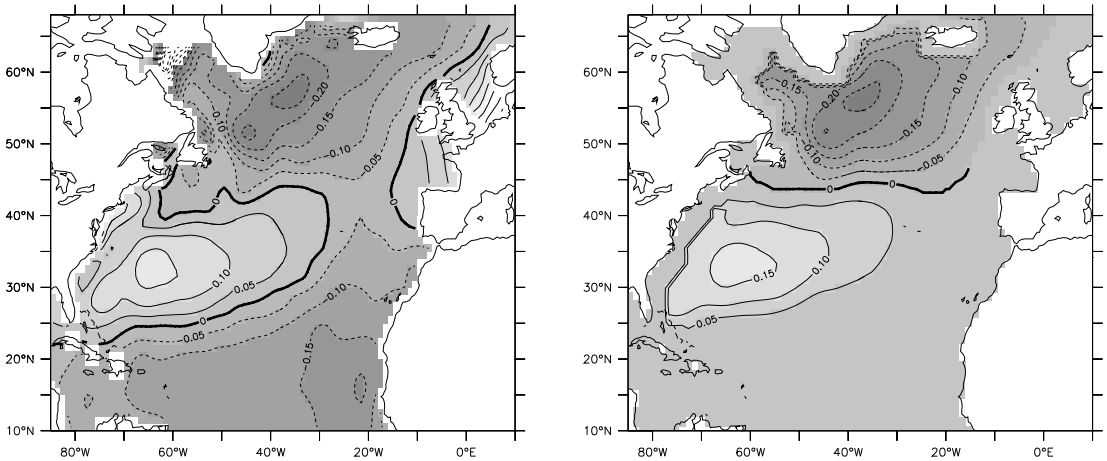

Figure 13: